P H Y S I C A L R E V I E W L E T T E R S

Density Affects the Nature of the Hexatic-Liquid Transition in Two-Dimensional Melting of Soft-Core Systems

Mengjie Zu, Jun Liu, Hua Tong, and Ning Xu[*]

*CAS Key Laboratory of Soft Matter Chemistry, Hefei National Laboratory for Physical Sciences at the Microscale,
and Department of Physics, University of Science and Technology of China, Hefei 230026, People's Republic of China*

We find that both continuous and discontinuous hexatic-liquid transitions can happen in the melting of two-dimensional solids of soft-core disks. For three typical model systems, Hertzian, harmonic, and Gaussian-core models, we observe the same scenarios. These systems exhibit reentrant crystallization (melting) with a maximum melting temperature T_m happening at a crossover density ρ_m. The hexatic-liquid transition at a density smaller than ρ_m is discontinuous. Liquid and hexatic phases coexist in a density interval, which becomes narrower with increasing temperature and tends to vanish approximately at T_m. Above ρ_m, the transition is continuous, in agreement with the Kosterlitz-Thouless-Halperin-Nelson-Young theory. For these soft-core systems, the nature of the hexatic-liquid transition depends on density (pressure), with the melting at ρ_m being a plausible transition point from discontinuous to continuous hexatic-liquid transition.

Two-dimensional melting is one of the most fascinating and puzzling phase transitions [1–3]. In contrast to the first-order nature in three dimensions, the possible existence of an intermediate phase between liquid and solid, e.g., the hexatic phase, confuses the nature of two-dimensional melting. According to the Kosterlitz-Thouless-Halperin-Nelson-Young (KTHNY) theory, the transitions from solid to hexatic and from hexatic to liquid are both continuous, accompanied by the disappearance of quasi-long-range positional and orientational orders, respectively [4–7]. Many experiments and simulations have confirmed the two-stage melting proposed by the KTHNY theory [8–17], while there are still exceptions [1,18–20]. The continuity of the hexatic-liquid transition also remains a matter of debate [21,22].

Recent studies have suggested that the nature of the hexatic-liquid transition is sensitive to the details of interparticle potential, including range, softness, length scale, and so on [14,23–25]. For instance, it has been confirmed that the hexatic-liquid transition of hard disks is first order [26–28]. In contrast, two-dimensional melting of ultrasoft Gaussian-core particles was claimed to be consistent with the KTHNY theory [23]. By tuning the exponent of the inverse power-law interparticle potential —and hence the particle softness—Kapfer and Krauth observed the intriguing evolution of the hexatic-liquid transition from discontinuous to continuous [25].

Consider a widely studied model system with finite range, purely repulsive, and soft-core particle interaction

$$U(r_{ij}) = \frac{\epsilon}{\alpha}\left(1 - \frac{r_{ij}}{\sigma}\right)^{\alpha}\Theta\left(1 - \frac{r_{ij}}{\sigma}\right),\qquad(1)$$

where r_{ij} is the separation between particles i and j, σ is the particle diameter, $\Theta(x)$ is the Heaviside function, ϵ is the characteristic energy scale, and α is a tunable parameter. At low temperatures and low densities, this system behaves as a hard sphere (disk) system [29]. Its melting temperature increases with density up to the maximum value T_m at a crossover density ρ_m. Above ρ_m, the melting temperature instead decreases with increasing density, exhibiting re-entrant crystallization (melting) [23,30–32]. As shown in Fig. 1 of the phase diagram for Hertzian repulsion ($\alpha = 5/2$) in two dimensions, multiple reentrant crystallizations with different crystal structures occur successively with increasing density. Therefore, both the hard and ultrasoft particle limits can be achieved with the same model, just by varying the density. It is then interesting to know whether both continuous and discontinuous hexatic-liquid transitions can occur in the same system.

By systematically studying the two-dimensional melting of Hertzian and harmonic ($\alpha = 2$) systems over a wide range of densities, we indeed observe both types of the hexatic-liquid transition. Interestingly, the crossover density ρ_m may act as the transition point between the two types. When $\rho < \rho_m$, the transition is discontinuous, showing the coexistence of liquid and hexatic phases. The density region of the coexistence decreases with increasing temperature and tends to vanish at T_m. When $\rho > \rho_m$, the transition is continuous. We further verify that the same scenario exists for the Gaussian-core model. Therefore, we propose that density affects the nature of the hexatic-liquid transition for soft-core particles exhibiting reentrant crystallization.

Our systems are rectangular boxes containing N disks with diameter σ and mass m. The systems have a side
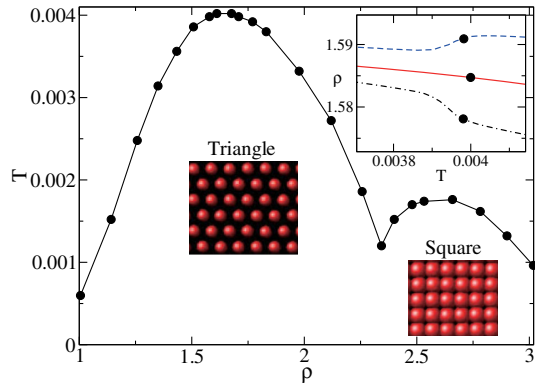
FIG. 1.   Phase diagram for $N = 1024$ Hertzian disks in the temperature T and density ρ plane. Here, we only show the density region with triangular and square solid structures. There are more structures at higher densities. The solid circles are approximate phase boundaries, above which are pure liquid states. The lines are a guide for the eye. The images for triangular and square structures are taken from simulation snapshots, with the particle diameters shown here being half of the actual values. (Inset) $\rho(T)$ curves across the transitions at $P = 0.12$ (dot dashed), 0.14 (solid), and 0.16 (dashed). The solid and dashed lines are shifted vertically by -0.06 and -0.117, respectively. The solid circles demonstrate how the phase boundaries in the main panel are determined.

length ratio $L_x : L_y = 2 : \sqrt{3}$ to accommodate the perfect triangular structure. Periodic boundary conditions are applied in both directions. We set the units of mass, energy, and length to be m, ϵ, and σ. The time is thus in units of $\sqrt{m\sigma^2/\epsilon}$. The temperature is in units of ϵ/k_B, with k_B being the Boltzmann constant. The density is calculated as $\rho = N\sigma^2/L_x L_y$.

The liquid, hexatic, and solid phases are identified from correlation functions of the bond-orientational and positional order parameters according to the KTHNY theory [14,21,23,33–35]:

$$g_6(r) = \langle \psi_6^*(\vec{r}_i)\psi_6(\vec{r}_j)\rangle, \tag{2}$$

$$g_G(r) = \langle e^{i\vec{G}\cdot(\vec{r}_i-\vec{r}_j)}\rangle, \tag{3}$$

where $r = |\vec{r}_i - \vec{r}_j|$ is the separation between particles i and j located at $\vec{r}_i$ and $\vec{r}_j$, respectively, $\vec{G}$ is the wave vector satisfying the periodic boundary conditions and at the first peak of the static structure factor, and $\langle . \rangle$ denotes the average over configurations and particles. The local bond-orientational order parameter ψ_6 for particle j is defined as

$$\psi_6(\vec{r}_j) = \frac{1}{n_j}\sum_{l=1}^{n_j} e^{i6\theta(\vec{r}_j-\vec{r}_l)}, \tag{4}$$

where the sum is over all n_j nearest neighbors of particle j determined by the Voronoi tessellation, and $\theta(\vec{r}_j - \vec{r}_l)$ is the angle between $\vec{r}_j - \vec{r}_l$ and a reference direction.

For the liquid phase, both $g_6(r)$ and $g_G(r)$ show exponential decay corresponding to short-range order. The hexatic phase has quasi-long-range bond-orientational order and short-range positional order, resulting in a power-law decay of $g_6(r)$, $g_6(r) \sim r^{-\eta_6}$ with $\eta_6 < 1/4$, and an exponential decay of $g_G(r)$. For the solid phase, $g_G(r) \sim r^{-\eta_G}$ with $\eta_G < 1/3$ and $g_6(r)$ shows almost no decay due to the quasi-long-range positional order and long-range bond-orientational order. In the Supplemental Material [36], we show some examples of the correlation functions and also the sub-block scaling analysis [37] to distinguish different phases.

We first study systems of Hertzian and harmonic repulsions. They have been widely employed in simulation and theoretical work and have been shown to approximate well interactions of various experimental systems such as poly(N-isopropylacrylamide) colloids, granular materials, and foams [38–40]. Both repulsions are soft core with positive definite Fourier transform [36], leading to reentrant crystallization [41]. Upon compression, there occurs a sequence of reentrant crystallizations with different solid structures [42]. In this Letter, we concentrate only on the first one with the triangular structure.

Figure 1 is obtained by quenching high-temperature $N = 1024$ states with a slow rate using constant-temperature and constant-pressure molecular dynamics simulations [43]. We have verified that our quench rate is slow enough that even slower quench rates will not change the phase diagram significantly. The phase diagram shows approximate locations of the phase boundaries, which slightly vary with system size due to finite size effects. The maximum melting temperature T_m for Hertzian (harmonic) repulsion estimated from the phase diagram is approximately 3.90×10^{-3} (7.10×10^{-3}) at a crossover density $\rho_m \approx 1.64$ (1.42) or pressure $P_m \approx 0.14$ (0.19) [36].

The inset to Fig. 1 shows the isobaric equation of state across the phase boundaries on both sides of and approximately at P_m. When $P < P_m$, the density jumps up across the transitions from liquid to solid. When $P > P_m$, the system exhibits a waterlike anomaly with the density of solid being lower than that of liquid. We find that the absolute value of the fast density change $|\Delta\rho_P|$ decreases when approaching P_m from either side. The melting at P_m may behave as a turning point with $\Delta\rho_P = 0$ [44]. As shown in the inset to Fig. 1, there is almost no sign of a density discontinuity when $P \approx P_m$ [45].

The melting at T_m looks special, at least for the continuity in density. It is interesting to figure out what role it plays in the two-dimensional melting of soft-core systems. To probe the details of the melting, we simulate much larger systems up to $N = 4 \times 10^5$ using a parallel LAMMPS package [46] in an $N\rho T$ or NPT ensemble and on both sides of ρ_m.

We calculate the equilibrium isothermal equation of state $P(\rho)$ in the $N\rho T$ ensemble across the transitions from solid
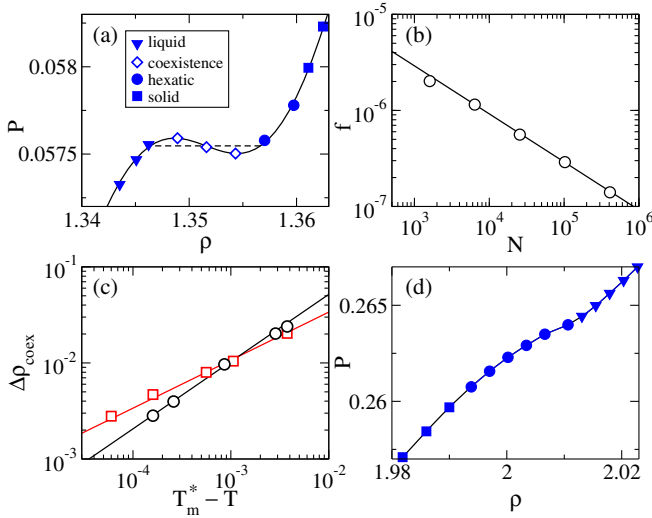
FIG. 2. (a) Isothermal equation of state $P(\rho)$ calculated at $T = 3.00 \times 10^{-3}$ across the melting at $\rho < \rho_m$ for $N = 102\,400$ Herztian disks. We use different symbols as explained in the legend to distinguish different states. The solid line is a tenth-order polynomial fit to the data. The dashed line demonstrates the Maxwell construction. (b) System size dependence of the interface free energy per particle f for Hertzian disks calculated at $T = 3.00 \times 10^{-3}$. The area encircled by the solid and dashed lines in (a) determines f. The line shows the scaling: $f \sim N^{-1/2}$. (c) Temperature dependence of the density interval of phase coexistence $\Delta\rho_{\text{coex}}$ for Herztian (circles) and harmonic (squares) repulsions. The lines show the scaling: $\Delta\rho_{\text{coex}} \sim (T_m^* - T)^{\gamma}$, with $T_m^* = 3.86 \times 10^{-3}$ (7.06×10^{-3}) and $\gamma = 0.70$ (0.50) for Herztian (harmonic) repulsion. (d) Isothermal equation of state $P(\rho)$ calculated for the same system and at the same temperature as (a), but across the transitions at $\rho > \rho_m$. The symbols have the same meaning as in (a). The line is a guide for the eye.

to liquid. Figure 2(a) shows $P(\rho)$ for $N = 102\,400$ Hertzian disks calculated at $T = 3.00 \times 10^{-3}$ and $\rho < \rho_m$. The curve displays a Mayer-Wood loop [47], characterizing phase coexistence. The loop is due to interface free energy between coexistent phases in finite size systems [48,49]. We fit the curve with a tenth-order polynomial and determine the boundaries of coexistence with the Maxwell construction. Seen from Fig. 2(a), it is the coexistence of hexatic and liquid phases because these two phases exist on both sides of the coexistence.

The interface free energy per particle f is calculated as half of the area encircled by the polynomial curve and the horizontal line of the Maxwell construction. With increasing system size, the Mayer-Wood loop flattens, so f tends to decrease with an increasing N. Figure 2(b) shows that $f \propto N^{-1/2}$, further demonstrating the discontinuous nature of the hexatic-liquid transition at $\rho < \rho_m$ [26,50].

Moreover, we find that the density interval of the phase coexistence $\Delta\rho_{\text{coex}}$ decreases with increasing temperature approaching T_m from the $\rho < \rho_m$ side. As shown in Fig. 2(c), $\Delta\rho_{\text{coex}}$ can be fitted well with a power-law

scaling relation: $\Delta\rho_{\text{coex}} \sim (T_m^* - T)^{\gamma}$, where T_m^* and γ are interaction dependent fitting parameters. The value of T_m^* used in Fig. 2(c) is 3.86×10^{-3} (7.06×10^{-3}) for Hertzian (harmonic) repulsion, in good agreement with the T_m estimated from the phase diagram. It is, thus, plausible to conjecture that the hexatic-liquid transition at T_m becomes continuous.

What may happen for melting at $\rho > \rho_m$? In Fig. 2(d), we show $P(\rho)$ at the same temperature as for Fig. 2(a), but on the higher density side of ρ_m. Across the transitions, P monotonically increases with ρ [51]. Therefore, the hexatic-liquid transition is continuous and agrees with the KTHNY theory. We have also verified that the same phenomenon occurs at all other temperatures.

In Fig. 3, we further compare the system size dependence of the isobaric density $\rho(T)$, the enthalpy $H(T)$, and the average bond-orientational order $\Psi_6(T) = \langle\psi_6(T)\rangle$ calculated in the NPT ensemble on both sides of P_m [52], where $\langle.\rangle$ denotes the average over particles and configurations. When $P < P_m$, all quantities apparently tend to be discontinuous with increasing system size, while they do not show such a tendency when $P > P_m$.

Figures 2 and 3 provide robust evidence to suggest that the hexatic-liquid transition undergoes a transition from discontinuous to continuous, with the melting at T_m being a possible transition point. In Sec. IV of the Supplemental Material [36], we provide further evidence by showing that the correlation length in the liquid phase tends to diverge approaching the maximum melting temperature from the
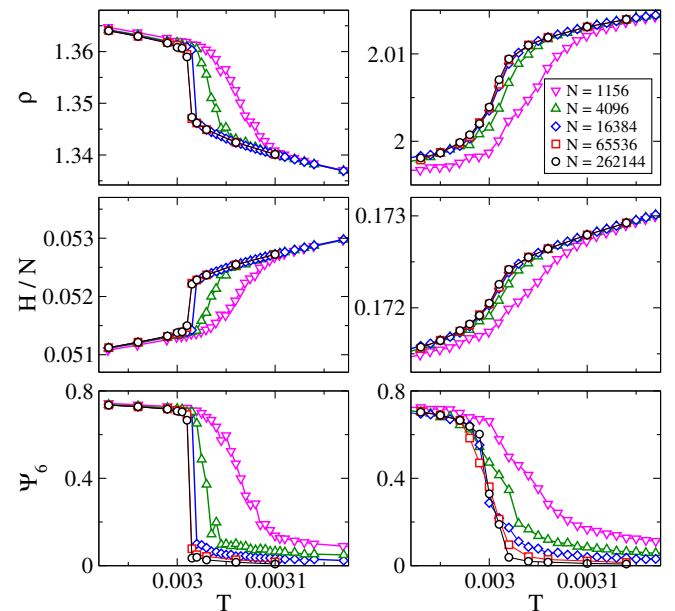
FIG. 3. System size dependence of the density $\rho(T)$, enthalpy per particle $H(T)/N$, and average bond-orientational order $\Psi_6(T)$ for Hertzian disks calculated at $P = 0.058$ $(< P_m$, left column) and 0.263 $(> P_m$, right column). The lines are a guide for the eye.
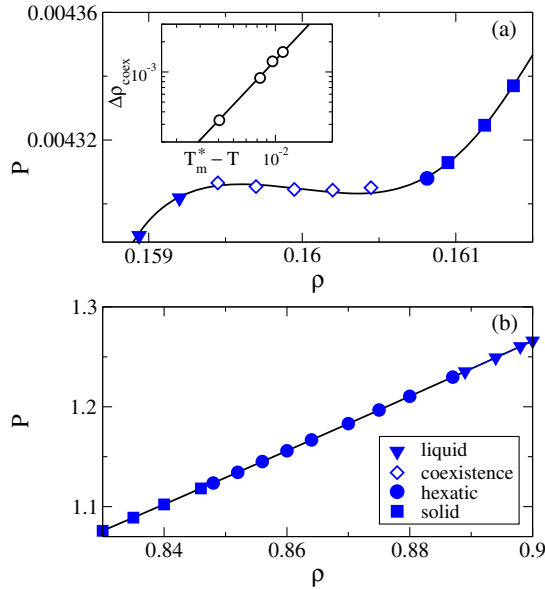
FIG. 4.   Isothermal equation of state $P(\rho)$ across the transitions for $N = 25\,600$ Gaussian-core disks calculated at $T = 1.80 \times 10^{-3}$ and at (a) $\rho < \rho_m$ and (b) $\rho > \rho_m$. The line in (a) is the tenth-order polynomial fit to the data, while in (b) is a guide for the eye. The legend in (b) explains the meaning of the symbols in both panels. The inset in (a) shows the temperature dependence of the density interval of phase coexistence $\Delta\rho_{coex}$. The data can be well fitted with $\Delta\rho_{coex} \sim (T_m^* - T)^\gamma$, where $T_m^* = 0.0114$ and $\gamma = 2.0$.

$\rho < \rho_m$ side. Two different types of hexatic-liquid transition can be achieved in the same system, just by tuning the density. Now there comes the question of whether the scenario is specific to systems described by Eq. (1) or exists in other soft-core systems. Next, we will examine the widely studied Gaussian-core model and show that our observations are not unique to Hertzian and harmonic repulsions.

The potential between interacting particles i and j for the Gaussian-core model is $U(r_{ij}) = \epsilon \exp(-r_{ij}^2/\sigma^2)$, with all parameters having the same meanings as in Eq. (1). We set a potential cutoff at $r_c = 4\sigma$ and shift the potential to make sure that both the potential and the force vanish at $r_{ij} \geq r_c$. We also use the same set of units as for Hertzian and harmonic systems. The Gaussian-core model exhibits re-entrant crystallization with maximum melting temperature $T_m \approx 0.011$ happening at $P_m \approx 0.16$ and $\rho_m \approx 0.37$ estimated from the phase diagram of $N = 1024$ systems [36].

Figure 4 compares isothermal $P(\rho)$ for Gaussian-core model calculated in the $N\rho T$ ensemble on both sides of ρ_m and at $T = 1.80 \times 10^{-3}$. Like Hertzian and harmonic repulsions, Fig. 4(a) shows that $P(\rho)$ at $\rho < \rho_m$ has a clear Mayer-Wood loop, so the hexatic-liquid transition here is discontinuous. The inset in Fig. 4(a) shows that the coexistent region $\Delta\rho_{coex}$ also decreases with increasing temperature and can be well fitted with $\Delta\rho_{coex} \sim (T_m^* - T)^\gamma$, where $T_m^* \approx 0.0114$ agrees well with T_m

estimated from the phase diagram. Again, for the Gaussian-core model, melting at T_m is likely to become continuous. In contrast, the continuity of the transitions above ρ_m is robust. The $P(\rho)$ curve at $\rho > \rho_m$ shown in Fig. 4(b) is rather straight across the melting with an almost density independent compressibility.

By studying three representative soft-core models exhibiting reentrant crystallization, we find that both continuous and discontinuous hexatic-liquid transitions happen in the same system. The type of the transition is determined by density. Our data suggest that the melting point at the maximum melting temperature may be the demarcation between the two types of transitions. Note that Hertzian and harmonic models are quite different from the Gaussian-core model [36], but they still behave similarly in the hexatic-liquid transition. Although it is impossible to check all models, based on our study, we are inclined to believe that our observations generalize to soft-core systems with reentrant crystallization. Anyhow, our study reveals the unknown extraordinary features of two-dimensional melting of soft-core systems, which can be tested in experimental systems such as star polymers [53].

In addition to the hexatic phase, the existence of the analogous tetratic phase upon the melting of solids with a square lattice structure has been reported and discussed [54–56]. However, compared to the hexatic phase, the tetratic phase is much less studied. One possible reason is that the square lattice structure is more difficult to form than the triangular lattice. Hertzian and harmonic models exhibit multiple reentrant crystallizations with various solid structures, which are ideal to investigate the tetratic phase and other intermediate phases. It would be interesting to know next whether we are able to observe different intermediate phases in these simple model systems and whether the melting of various types of solids follows similar scenarios or not.

*ningxu@ustc.edu.cn
[1] K. L. Strandburg, Rev. Mod. Phys. **60**, 161 (1988).
[2] J. G. Dash, Rev. Mod. Phys. **71**, 1737 (1999).
[3] U. Gasser, J. Phys. Condens. Matter **21**, 203101 (2009).
[4] J. M. Kosterlitz and D. J. Thouless, J. Phys. C **6**, 1181 (1973).
[5] D. R. Nelson and B. I. Halperin, Phys. Rev. B **19**, 2457 (1979).

[6] B. I. Halperin and D. R. Nelson, Phys. Rev. Lett. **41**, 121 (1978).

[7] A. P. Young, Phys. Rev. B **19**, 1855 (1979).

[8] C. A. Murray and D. H. Van Winkle, Phys. Rev. Lett. **58**, 1200 (1987).

[9] K. Zahn, R. Lenke, and G. Maret, Phys. Rev. Lett. **82**, 2721 (1999).

[10] H. H. von Grünberg, P. Keim, K. Zahn, and G. Maret, Phys. Rev. Lett. **93**, 255703 (2004).

[11] P. Keim, G. Maret, and H. H. von Grünberg, Phys. Rev. E **75**, 031402 (2007).

[12] B. J. Lin and L. J. Chen, J. Chem. Phys. **126**, 034706 (2007).

[13] S. Z. Lin, B. Zheng, and S. Trimper, Phys. Rev. E **73**, 066106 (2006).

[14] S. I. Lee and S. J. Lee, Phys. Rev. E **78**, 041504 (2008).

[15] W. K. Qi, Z. Wang, Y. Han, and Y. Chen, J. Chem. Phys. **133**, 234508 (2010).

[16] S. Prestipino, F. Saija, and P. V. Giaquinta, J. Chem. Phys. **137**, 104503 (2012).

[17] H. Shiba, A. Onuki, and T. Araki, Europhys. Lett. **86**, 66004 (2009).

[18] C. Alba-Simionesco, B. Coasne, G. Dosseh, G. Dudziak, K. E. Gubbins, R. Radhakrishnan, and M. Sliwinska-Bartkowiak, J. Phys. Condens. Matter **18**, R15 (2006).

[19] S. T. Chui, Phys. Rev. Lett. **48**, 933 (1982).

[20] Y. Lansac, M. A. Glaser, and N. A. Clark, Phys. Rev. E **73**, 041501 (2006).

[21] P. Bladon and D. Frenkel, Phys. Rev. Lett. **74**, 2519 (1995).

[22] A. H. Marcus and S. A. Rice, Phys. Rev. Lett. **77**, 2577 (1996).

[23] S. Prestipino, F. Saija, and P. V. Giaquinta, Phys. Rev. Lett. **106**, 235701 (2011).

[24] D. E. Dudalov, Yu. D. Fomin, E. N. Tsiok, and V. N. Ryzhov, J. Phys. Conf. Ser. **510**, 012016 (2014).

[25] S. C. Kapfer and W. Krauth, Phys. Rev. Lett. **114**, 035702 (2015).

[26] E. P. Bernard and W. Krauth, Phys. Rev. Lett. **107**, 155704 (2011).

[27] M. Engel, J. A. Anderson, S. C. Glotzer, M. Isobe, E. P. Bernard, and W. Krauth, Phys. Rev. E **87**, 042134 (2013).

[28] W. Qi, A. P. Gantapara, and M. Dijkstra, Soft Matter **10**, 5449 (2014).

[29] N. Xu, T. K. Haxton, A. J. Liu, and S. R. Nagel, Phys. Rev. Lett. **103**, 245701 (2009); X. Wang, W. Zheng, L. Wang, and N. Xu, Phys. Rev. Lett. **114**, 035502 (2015).

[30] E. A. Jagla, J. Chem. Phys. **111**, 8980 (1999).

[31] A. B. de Oliveira, P. A. Netz, T. Colla, and M. C. Barbosa, J. Chem. Phys. **124**, 084505 (2006).

[32] Yu. D. Fomin, N. V. Gribova, V. N. Ryzhov, S. M. Stishov, and D. Frenkel, J. Chem. Phys. **129**, 064512 (2008).

[33] K. Binder, S. Sengupta, and P. Nielaba, J. Phys. Condens. Matter **14**, 2323 (2002).

[34] S. V. Buldyrev, G. Malescio, C. A. Angell, N. Giovambattista, S. Prestipino, F. Sajia, H. E. Stanley, and L. Xu, J. Phys. Condens. Matter **21**, 504106 (2009).

[35] P. Vilaseca and G. Franzese, J. Non-Cryst. Solids **357**, 419 (2011).

[36] See Supplemental Material at http://link.aps.org/supplemental/10.1103/PhysRevLett.117.085702 for additional information about the criterion of reentrant crystallization, some results for harmonic and Gaussian-core models, more supporting information for the Hertzian model, and the identification and the visualization of different phases.

[37] K. Bagchi, H. C. Andersen, and W. Swope, Phys. Rev. Lett. **76**, 255 (1996).

[38] Z. Zhang, N. Xu, D. T. N. Chen, P. Yunker, A. M. Alsayed, K. B. Aptowicz, P. Habdas, A. J. Liu, S. R. Nagel, and A. G. Yodh, Nature (London) **459**, 230 (2009).

[39] T. S. Majmudar, M. Sperl, S. Luding, and R. P. Behringer, Phys. Rev. Lett. **98**, 058001 (2007).

[40] K. W. Desmond, P. J. Young, D. Chen, and E. R. Weeks, Soft Matter **9**, 3424 (2013).

[41] C. N. Likos, A. Lang, M. Watzlawek, and H. Löwen, Phys. Rev. E **63**, 031206 (2001).

[42] W. L. Miller and A. Cacciuto, Soft Matter **7**, 7552 (2011).

[43] Our phase diagram shows exactly the first two regions below $\rho < 3$ in Fig. 2 of Ref. [42]. Because of low data resolution, the maximum of the melting curve for the square solid structure does not show up in Fig. 2 of Ref. [42].

[44] P. Bolhuis, M. Hagen, and D. Frenkel, Phys. Rev. E **50**, 4880 (1994).

[45] As discussed in Sec. III of the Supplemental Material [36], even though $\Delta \rho_P \approx 0$ at $P \approx P_m$, there is still a thin layer of the hexatic phase between solid and liquid.

[46] See http://lammps.sandia.gov/.

[47] J. E. Mayer and W. W. Wood, J. Chem. Phys. **42**, 4268 (1965).

[48] H. Furukawa and K. Binder, Phys. Rev. A **26**, 556 (1982).

[49] M. Schrader, P. Virnau, and K. Binder, Phys. Rev. E **79**, 061104 (2009).

[50] J. Lee and J. M. Kosterlitz, Phys. Rev. Lett. **65**, 137 (1990).

[51] As shown in Fig. S5(b) of the Supplemental Material [36], the system size effects are already small for the largest systems studied, so it is plausible to expect that the Mayer-Wood loop and the phase coexistence observed at $\rho < \rho_m$ do not occur.

[52] Refer to Fig. S3 of the Supplemental Material [36] for a phase diagram in the T-P plane.

[53] M. Watzlawek, C. N. Likos, and H. Löwen, Phys. Rev. Lett. **82**, 5289 (1999).

[54] T. Terao, J. Chem. Phys. **139**, 134501 (2013).

[55] K. W. Wojciechowski and D. Frenkel, Computational Methods in Science and Technology **10**, 235 (2004).

[56] Y. Peng, Z. Wang, A. M. Alsayed, A. G. Yodh, and Y. Han, Phys. Rev. Lett. **104**, 205703 (2010).